Archives of Current Medical Research
Arch Curr Med Res 2026; 7(1): 179-188

Received: 14 June 2025
Revised: 06 September 2025
Accepted: 16 November 2025
DOI: 10.47482/acmr.1719683

ORIGINAL ARTICLE

Epidemiology of the Talus Osteochondral Lesions: An MRI Survey in 490 Patients

Fırat Doğruöz[1] Murat Yuncu[2] Mehmet Barış Ertan[3] Koray Kaya Kılıç[4] Aliekber Yapar[1] Özkan Köse[1]

1 University of Health Sciences, Antalya Training and Research Hospital, Department of Orthopedics and Traumatology, Antalya, Türkiye
2 Elmali State Hospital, Department of Orthopedics and Traumatology, Antalya, Türkiye
3 Private Medikum Hospital, Orthopaedics and Traumatology Clinic, Antalya, Türkiye
4 University of Health Sciences, Antalya Training and Research Hospital, Department of Radiology, Antalya, Türkiye

Abstract

Background: Osteochondral lesions of the talus (TOLs) are a frequent cause of chronic ankle pain and functional limitation. Despite their clinical significance, data on their prevalence, anatomical distribution, and morphological features remain limited, particularly concerning sex-based differences.

Methods: This retrospective study reviewed 5,356 ankle MRI scans performed over five years to identify patients with TOLs. 490 skeletally mature patients (283 females, 207 males) were included. Lesions were evaluated based on anatomical localization using a standardized nine-zone grid, graded according to the Bristol/Hepple classification, and measured using region of interest (ROI) tools. Inter- and intra-observer reliability was assessed using ICC and Cohen's kappa statistics.

Results: The overall prevalence of TOLs was 9.1%, with similar rates in males (9.3%) and females (9.0%). The mean age was 46.2±14.3 years. Lesions were most commonly located in Zones 4 (33.7%) and 7 (33.5%). The mean lesion area was 78.2±61.9 mm², with the largest lesions in Zone 4. Grade 1 (26.2%) and Grade 5 (20.70%) were the most frequent lesion grades. Male patients were significantly younger(42,2) and had larger lesions ($p<0.01$), whereas bilateral involvement and medial localization were more common in females ($p<0.05$).

Conclusion: This study provides the first large-scale MRI-based analysis integrating zonal lesion mapping with sex-specific morphological characteristics of TOLs. The findings highlight medial talar dome vulnerability and reveal sex-related differences in lesion presentation, suggesting distinct pathomechanical pathways. These results may aid in early diagnosis and guide personalized management strategies for TOLs.

Keywords: Talus osteochondral lesions, incidence, epidemiology, osteochondritis dissecans, Hepple classification.

Corresponding Author:
Aliekber Yapar, MD
Department of Orthopaedic and Traumatology, Antalya Training and Research Hospital, Antalya, Türkiye
Email: aliekberyapar@hotmail.com

INTRODUCTION

Osteochondral lesions of the talus (TOLs) represent a significant source of chronic ankle pain and functional limitation, particularly among active individuals. These lesions involve damage to the articular cartilage and underlying subchondral bone of the talar dome, typically manifesting with pain, swelling, and restricted range of motion (1). TOLs may arise following acute trauma, repetitive microtrauma, or ischemic events such as osteonecrosis (2,3). Although TOLs are frequently encountered in clinical practice, their true prevalence in the general population remains uncertain. Reported prevalence varies between 7–10% in general orthopedic populations, and may reach up to 45% in patients with ankle fractures. Most existing data derive from symptomatic cohorts, and little is known about the influence of sex on lesion characteristics or distribution (4). Accurately estimating epidemiological parameters is further complicated by the often asymptomatic nature of these lesions and the reliance on MRI for definitive diagnosis.

This study does not aim to determine the incidence of TOLs. Rather, it provides a descriptive analysis of lesion characteristics in a large cohort of patients who underwent ankle MRI for pain-related symptoms over a five-year period. Specifically, we sought to evaluate the anatomical distribution and size of the lesions using a standardized nine-zone grid system and to assess their classification based on MRI grading. In addition, we explored potential associations between lesion location, size, and grade, and examined whether these parameters differed between male and female patients (5).

We hypothesize that lesion characteristics—particularly size and grade—may vary according to their anatomical location, and that clinically relevant sex-based differences may exist. By addressing these questions in a large, well-defined cohort, this study aims to enhance the understanding of TOL morphology and distribution, and to inform clinical decision-making regarding diagnosis, prognosis, and treatment planning.

MATERIALS AND METHODS

Patients and Study Design

A retrospective review was conducted on skeletally mature patients (aged >18 years) who presented to the authors' institution with ankle-related complaints and underwent magnetic resonance imaging (MRI) between January 2018 and December 2022. MRI reports were systematically screened for indicators of talus osteochondral lesions (TOL) using the following search terms: osteochondritis dissecans, osteochondral defect, osteochondral lesion, talar bone marrow edema, talar subchondral cyst, and talar cartilage lesion, as well as the abbreviations TOL, OCD (osteochondritis dissecans), and OLT (osteochondral lesion of talus). During the five-year study period, 5,356 ankle MRI reports (2,219 males and 3,137 females) were reviewed. Of these, 531 patients were initially identified with a potential diagnosis of TOL. A musculoskeletal radiologist re-evaluated the MRI examination, and patients were excluded if they had a prior history of ankle surgery, radiographic evidence of ankle osteoarthritis, or incomplete clinical or imaging data. After applying the exclusion criteria, 490 patients with a confirmed diagnosis of TOL were included in the final analysis. This study followed the ethical principles outlined in the Declaration of Helsinki (1964) and its subsequent revisions. The study protocol was approved by the Institutional Review Board (01/16, 06.01.2022).

Radiological Assessment and Measurements

All MRI examinations were performed using a 1.5 Tesla Achieva DS Advance system (Philips Healthcare, Eindhoven, The Netherlands) equipped with an 8-channel ankle coil, with the ankle positioned in neutral alignment. The imaging protocol followed standard clinical routines and included proton density-weighted (PDw) spectral presaturation inversion recovery (SPIR) sequences, T1-weighted turbo spin-echo (TSE) sequences, and T2-weighted SPIR sequences. Images were transferred to a picture archiving and communication system (PACS) workstation (Sectra IDS7, Version 18.2; Sectra AB) for evaluation.

A musculoskeletal radiologist and an orthopedic surgeon independently reviewed MR images. Each observer performed the radiologic assessments randomly on two separate occasions, with a minimum interval of three weeks between assessments. Observers were blinded to their prior evaluations and to those of the other reviewer to reduce bias. Lesion location was de-

termined using the 9-zone anatomical grid described by Raikin et al. (6). When a lesion extended across multiple zones, the zone with the largest area of involvement was designated as the primary location (Figure 1). Lesion grading was performed according to the Bristol/Hepple MRI classification system (7) (Table 1) . Lesion size was measured on the most caudal axial slice using the region of interest (ROI) tool within the PACS software. The total lesion area included the osteochondral defect and associated bone marrow edema (Figure 2).

After completing the measurements, inter- and intra-observer reliability was assessed. Intraclass correlation coefficients (ICCs) with 95% confidence intervals (CIs) were calculated for continuous variables. A two-way random-effects model was employed to evaluate inter-observer reliability, accounting for absolute agreement and consistency. ICC values were interpreted according to established benchmarks: poor (<0.50), moderate (0.50–0.75), good (0.75–0.90), and excellent (>0.90) (8). For categorical variables, such as lesion grade and location, reliability was assessed using Cohen's kappa statistic with 95% CIs. Kappa values were interpreted as follows: poor (<0.00), slight (0.00–0.20), fair (0.21–0.40), moderate (0.41–0.60), substantial (0.61–0.80), and almost perfect (0.81–1.00) (9). The reliability of measurements was excellent (more than >0.800) for all measurements (Table 2). Observers reached a final grade and location rating by consensus on discordant cases through a discussion session. The mean of lesion size measurements and the consensus decision on the location and grade of the lesion were used for the final analysis.

Statistical Analysis

Descriptive statistics were used to summarize patient demographics and radiological findings. Group comparisons between sexes were performed using the student's t-test for continuous variables and the Chi-square test for categorical variables. A p-value < 0.05 was considered indicative of statistical significance.

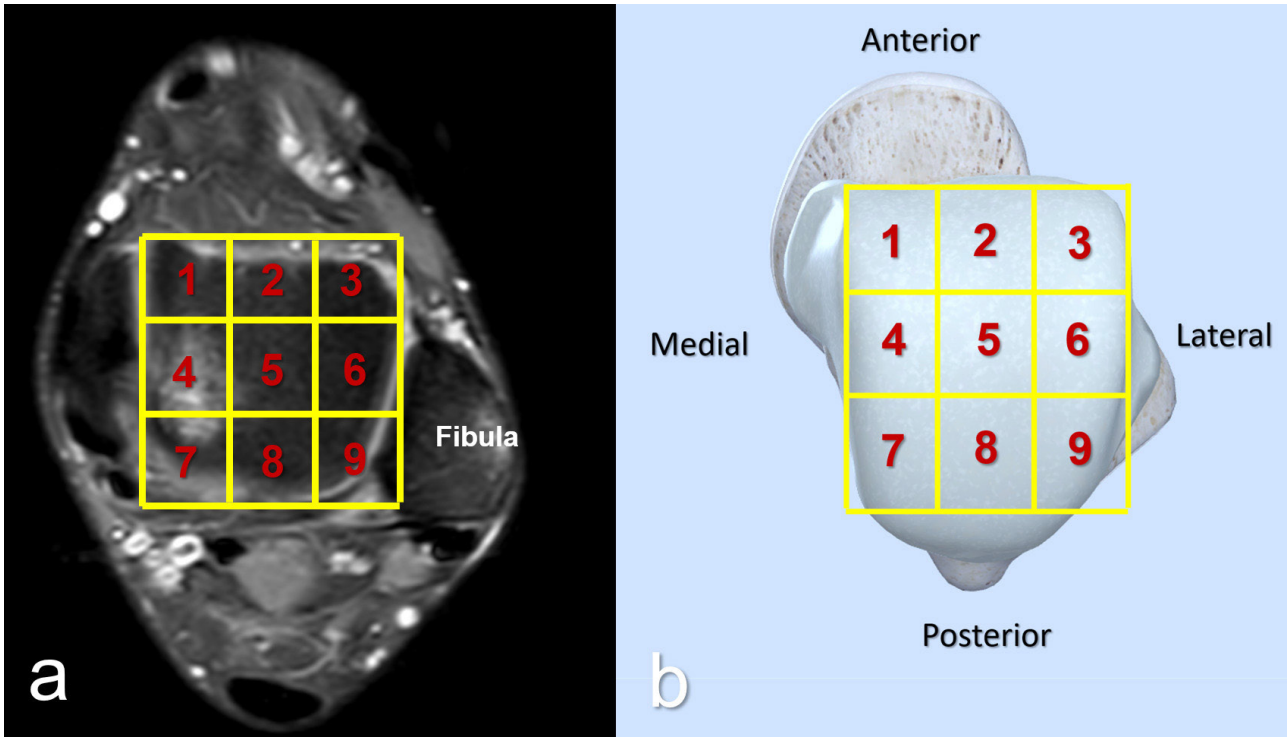

Figure 1: Nine-zone anatomical grid system for localizing osteochondral lesions of the talus.
(a) Axial MRI view and (b) schematic representation of the talar dome, divided into a 3×3 grid based on the method described by Raikin et al. Zones are numbered from 1 to 9, proceeding left to right and top to bottom. This system allows standardized reporting of lesion location.

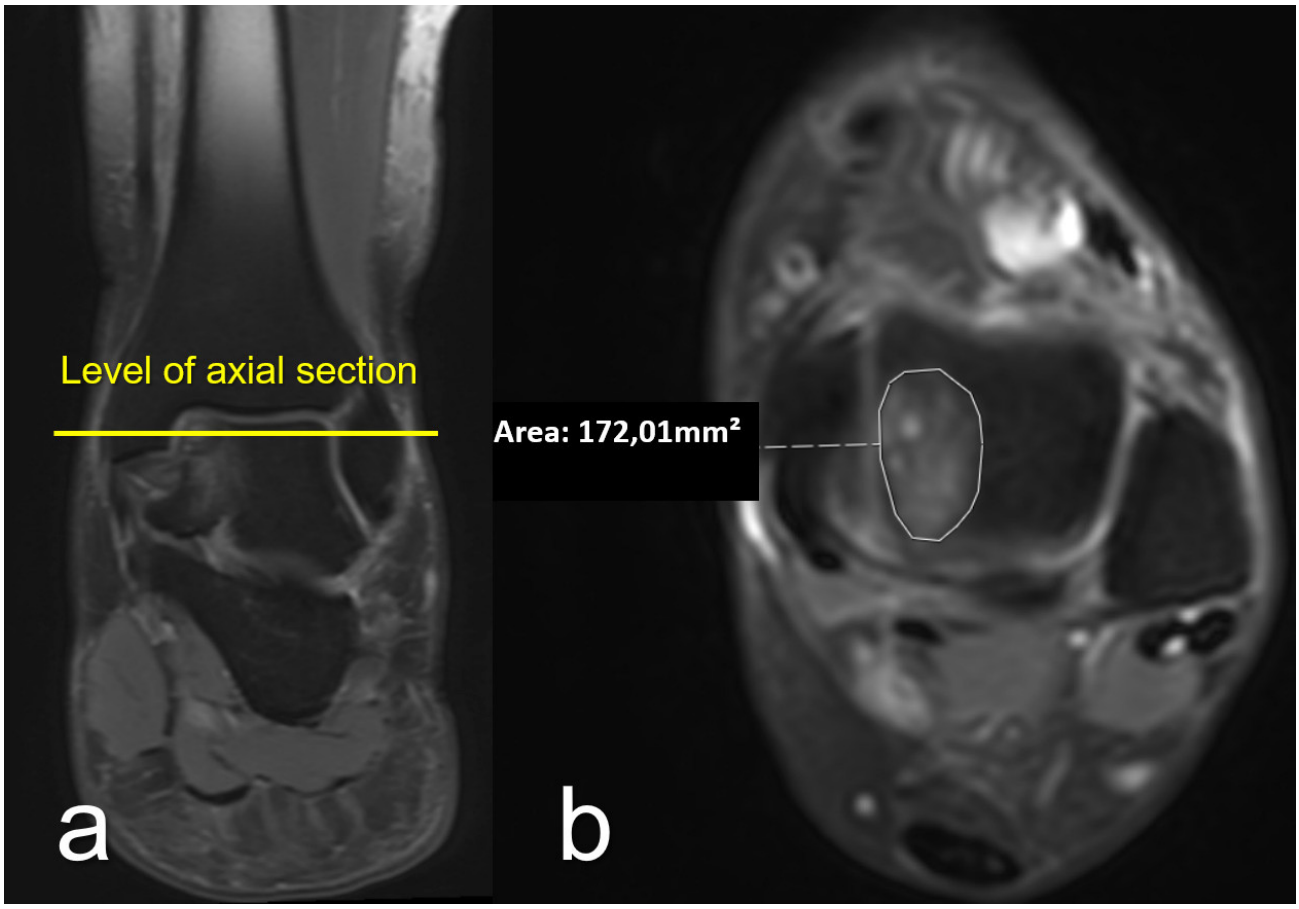

Figure 2: Measurement of osteochondral lesion size on axial MRI. (a) Coronal MRI showing the level of the most caudal axial slice used for measurement. (b) Axial proton density-weighted MRI image with spectral presaturation inversion recovery (SPIR) showing the outlined lesion area. Lesion size was calculated using the region of interest (ROI) tool, including both the osteochondral defect and surrounding bone marrow edema. The measured area in this example is 172.01 mm².

Table 1. Hepple Classification of Talus Osteochondral Lesions Using Magnetic Resonance Imaging

Grade	Findings
1	Articular cartilage injury only
2A	Cartilage injury with bony fracture and edema (Flap, acute)
2B	Cartilage injury without bony fracture and edema (Chronic)
3	Detached, non-displaced bony fragment (Fluid rim beneath the fragment)
4	Displaced fragment, uncovered subchondral bone
5	Subchondral cyst present

Table 2. Results of Reliability Analysis

Variables	Reliability analysis		ICC / Kappa	95% CI	Interpretation
Grid Location	**Intra-observer reliability**				
	Observer A t_1	*Observer A* t_2	0.9391	0.913-0.963	Excellent
	Observer B t_1	*Observer B* t_2	0.9791	0.961-0.994	Excellent
	Inter-observer reliability				
	Observer A t_1	*Observer B* t_1	0.9241	0.894-0.954	Excellent
	Observer A t_2	*Observer B* t_2	0.9331	0.904-0.960	Excellent
Area (mm^2)	**Intra-observer reliability**				
	Observer A t_1	*Observer A* t_2	0.9792	0.975-0.983	Excellent
	Observer B t_1	*Observer B* t_2	0.9832	0.980-0.986	Excellent
	Inter-observer reliability				
	Observer A t_1	*Observer B* t_1	0.9652	0.943-0.986	Excellent
	Observer A t_2	*Observer B* t_2	0.9592	0.948-0.970	Excellent
MRI Grade	**Intra-observer reliability**				
	Observer A t_1	*Observer A* t_2	0.8441	0.809-0.879	Excellent
	Observer B t_1	*Observer B* t_2	0.8921	0.863-0.921	Excellent
	Inter-observer reliability				
	Observer A t_1	*Observer B* t_1	0.9281	0.903-0.953	Excellent
	Observer A t_2	*Observer B* t_2	0.9421	0.919-0.965	Excellent

[1] Kappa statistics, [2]ICC, Abbreviations, ICC: Interclass correlation coefficient, CI: Confidence interval, t_1 : First assessment, t_2 : Second assessment, MRI : Magnetic resonance imaging

RESULTS

490 patients with TOL out of 5,356 ankle MRI scans were identified, giving an overall prevalence of 9.1% (9.0% in females, 9.3% in males). The mean age of the patients was 46.2±14.3 years (range, 18-88 years). Of the 490 patients, 283 (57.8%) were female, and the remaining 207 (42.2%) were male. 26 patients had bilateral involvement; thus, 516 feet [272 (52.7%) right and 244 (47.3%) left] were evaluated.

Lesions were located most commonly in Zone 4 (33.7%) and Zone 7 (33.5%), followed by Zone 1 (11.0%). The mean articular surface involvement was 78.2±61.9 mm2 (range 4.78-367.6 mm2), and the largest involvement

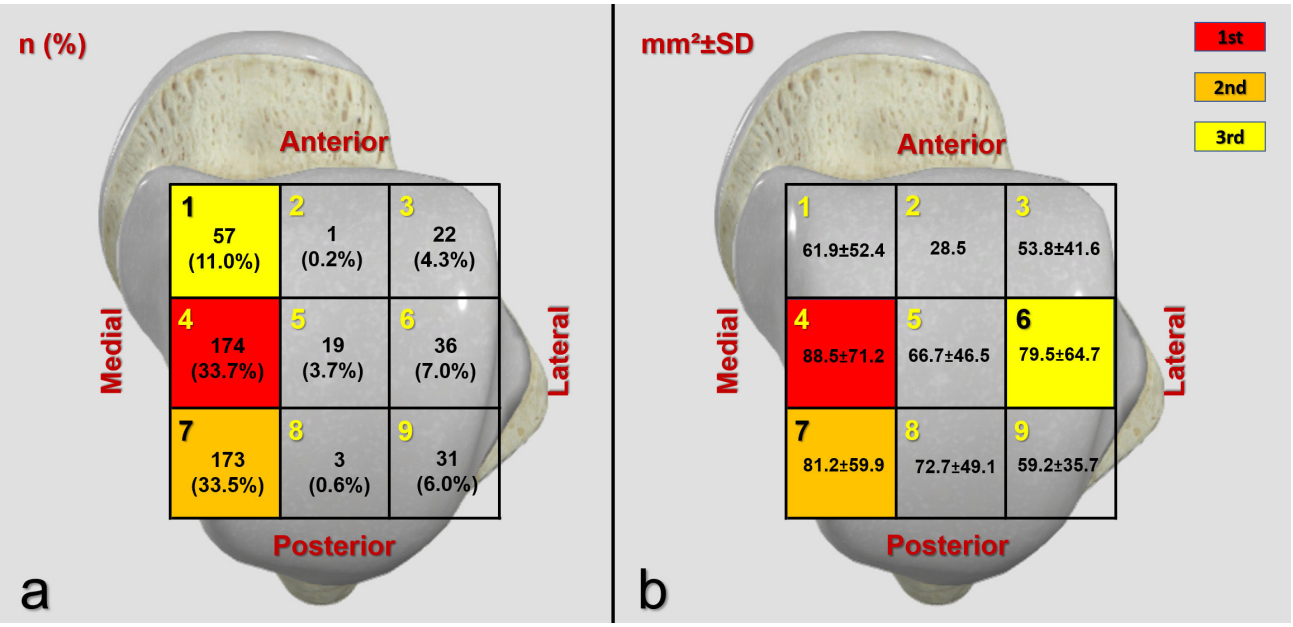

Figure 3: Distribution and size of talar osteochondral lesions by anatomical zone. (a) Frequency and percentage of lesions within each of the nine zones. (b) Mean lesion area (mm² ± standard deviation) by zone. Zones 4 and 7 were the most frequently affected regions, while the largest mean lesion size was observed in Zone 4. Color coding indicates the top three most commonly involved zones (1st = red, 2nd = orange, 3rd = yellow).

Table 3. Grade of the Lesions and Their Frequencies

Grade	Frequency (n)	Percent (%)
Grade 1	135	26.2
Grade 2A	105	20.3
Grade 2B	74	14.3
Grade 3	37	7.2
Grade 4	58	11.2
Grade 5	107	20.7
Total	516	100

Table 4. Comparison of Lesion Characteristics Between Genders

Variables	Male *(n:207)*	Female *(n:283)*	p-value
Age (years±SD)	43.9±14.7	47.9±13.7	0.002[1]
Side (n, %)			0.210[2]
Right	116 (56%)	147 (51.9%)	
Left	91 (44%)	136 (48.1%)	
Bilaterality (n, %)			0.031[2]
Yes	6 (2.9%)	20 (7.1%)	
No	201 (97.1%)	263 (92.9%)	
Area (mm2±SD)	90.2±69.9	69.6±56.3	0.001[1]
Location (n, %)			0.002[2]
Medial lesions	145 (70%)	236 (83.4%) *	
Central lesions	10 (4.8%)	10 (3.5%)	
Lateral lesions	52 (25.1%) *	37 (13.1%)	
Grade (n, %)			0.001[2]
Grade 1	41 (19.8%)	88 (31.1%) *	
Grade 2A	34 (16.4%)	66 (23.3%)	
Grade 2B	38 (18.4%)	34 (12%)	
Grade 3	18 (8.7%)	18 (6.4%)	
Grade 4	31 (15.0%) *	19 (6.7%)	
Grade 5	45 (21.7%)	58 (20.5%) *	

*[1]Student t-test [2]Chi-square test *Adjusted residual >-2.0*

was observed in Zone 4 (Figure 3). The most commonly observed grade of the lesion was Grade 1 [135 (26.2%)], followed by Grade 5 [107 (20.7.0%)] (Table 3).

Male patients were younger than female patients (p=0.001), and the lesion size was larger in male patients (p=0.002). Bilateral involvement was more common in female patients; however, the difference was not statistically significant (p=0.101). Table 4 presents a comparative analysis between genders.

DISCUSSION

This study presents a comprehensive analysis based on the review of 5,356 ankle MRI scans, identifying 490 patients with osteochondral lesions of the talus (TOLs). The overall prevalence of TOLs was 9.1%, which is consistent with previously reported rates ranging from 7% to 10% in general orthopedic populations (4). However, markedly higher prevalence has been reported in selected groups; for instance, Martijn et al. noted an incidence of 45% in patients with ankle fractures, and similarly elevated rates have been documented in populations with high physical demands, such as military personnel (10). This variability underscores the influence of patient demographics, trauma history, and imaging techniques on reported prevalence rates (3,11).

In our cohort, a slightly higher prevalence was observed in males (9.3%) compared to females (9.0%). The mean age of patients was 46.2 years, indicating that TOLs predominantly affect a middle-aged demographic. Notably, male patients were significantly younger than female patients and exhibited larger lesion sizes. These findings may suggest sex-specific differences in the development or progression of TOLs, potentially influenced by biomechanical factors, activity levels, or hormonal profiles. By offering detailed data on lesion prevalence, anatomical distribution, size, and MRI-based grading, this study contributes valuable information to the limited literature on TOLs. It has important implications for their diagnosis and management.

In this cohort, most osteochondral lesions were localized to the medial aspect of the talus, with over two-thirds occurring in Zones 4 and 7. This distribution aligns with findings from previous anatomical and imaging-based mapping studies. For instance, Diepen et al., in a systematic review encompassing more than 2,000 patients with TOLs, reported that 59% of lesions were located in the posteromedial and centromedial regions of the talar dome (12). Similarly, Raikin et al. identified the medial talar dome as the most frequently affected site (13). The predominance of medial lesions is likely explained by the biomechanical forces acting on the talus during standard injury mechanisms, particularly inversion and plantarflexion, which place increased stress on the medial talar dome (14).

A noteworthy aspect of our findings is the observed sex-based variation in lesion characteristics. Male patients were significantly younger and demonstrated larger lesion areas than female patients. This may reflect a higher exposure to high-energy trauma or greater participation in physically demanding sports activities among males (10). Conversely, female patients exhibited a higher incidence of bilateral lesions and a predilection for medial talar involvement. These patterns may be influenced by sex-specific factors such as hormonal profiles, anatomical differences, or increased ligamentous laxity. Supporting this, Kessler et al. reported a higher incidence of osteochondritis dissecans in adolescent females (mean age ~13 years) than their male counterparts in pediatric populations—a trend consistent with the present findings (15).

The bimodal distribution observed in lesion grading—characterized by the predominance of Grade 1 and Grade 5 lesions—suggests the coexistence of early-stage, often asymptomatic presentations and advanced degenerative changes. This pattern is consistent with the classification framework proposed by van Dijk and Kennedy (14). Grade 1 lesions are typically amenable to conservative management and may remain asymptomatic or resolve over time, whereas Grade 5 lesions frequently require surgical intervention, including osteochondral autograft or allograft transplantation due to extensive subchondral damage.

Our MRI-based regional mapping of lesion characteristics aligns with the revised classification system introduced by Hepple et al., which highlights the value of high-resolution MRI in evaluating critical prognostic parameters such as lesion stability, intra-lesional con-

tent, and subchondral cyst formation (7). While MRI remains the gold standard for diagnosing osteochondral lesions, computed tomography (CT) is a useful adjunct in preoperative planning, particularly in cases involving complex fracture patterns or suspected coexisting tibial pathology (13,15). Irwin et al. reported that older patients with lateral talar lesions are more likely to present with concomitant tibial osteochondral involvement. This factor may significantly influence joint preservation strategies and long-term outcomes (16).

The predominance of medial talar lesions in non-traumatic cases observed in this study contrasts with findings from acute fracture scenarios. Togher and Martijn reported no significant zonal predilection in patients with ankle fractures, attributing this variability to differences in fracture classification systems and the timing of imaging acquisition (10,15,17). These discrepancies suggest that lesion localization may be influenced by the initial injury mechanism, chronic loading patterns, and post-traumatic joint adaptation over time15. Moreover, our findings support previous observations by Orr et al., who reported a rising incidence of TOLs over time, particularly among military populations (11). This trend is likely multifactorial, reflecting increased MRI utilization, improved clinical recognition, and demographic risk factors such as female sex, Caucasian ethnicity, and age over 20 years.

Third, although previously noted as a limitation, inter-observer reliability for lesion grading was in fact analyzed and found to be excellent (Kappa = 0.928 and 0.942).

This study offers valuable insights into the prevalence, anatomical distribution, and morphological characteristics of talar osteochondral lesions (TOLs) within a large and heterogeneous patient population. The predominance of lesions in the medial talar dome, particularly within Zones 4 and 7, reinforces the concept of regional anatomical vulnerability. Additionally, the observed sex-based differences in lesion size, laterality, and localization suggest distinct pathomechanical and demographic influences, underscoring the need for further investigation. Magnetic resonance imaging remains the cornerstone for diagnosing and staging TOLs; however, computed tomography should be considered a complementary tool during preoperative planning, particularly in complex or ambiguous cases. Future research should aim to correlate imaging-based findings with clinical outcomes and explore longitudinal data across diverse age groups and activity profiles. This is the first study to combine zonal MRI-based lesion mapping with sex-specific analyses in a large and demographically diverse cohort. These findings provide new perspectives on anatomical susceptibility and may inform more individualized diagnostic and therapeutic strategies. Ultimately, this information has the potential to enhance early detection and guide surgical decision-making in the management of talar osteochondral lesions.

REFERENCES

1. Bruns J, Habermann C, Werner M. Osteochondral Lesions of the Talus: A Review on Talus Osteochondral Injuries, Including Osteochondritis Dissecans. Cartilage. 2021 Dec;13(1_suppl):1380S-1401S.
2. Savage-Elliott I, Ross KA, Smyth NA, Murawski CD, Kennedy JG. Osteochondral lesions of the talus: a current concepts review and evidence-based treatment paradigm. Foot Ankle Spec. 2014;7(5):414-22.
3. Mangwani J, Brockett C, Pegg E. Osteochondral lesions of talus. Bone Joint Res. 2024;13(12):790-792.
4. Orr JD, Dawson LK, Garcia EJ, Kirk KL. Incidence of osteochondral lesions of the talus in the United States military. Foot Ankle Int. 2011;32(10):948-54.
5. Elias I, Raikin SM, Schweitzer ME, Besser MP, Morrison WB, Zoga AC. Osteochondral lesions of the distal tibial plafond: localization and morphologic characteristics with an anatomical grid. Foot Ankle Int. 2009;30(6):524-9.
6. Raikin SM, Elias I, Zoga AC, Morrison WB, Besser MP, Schweitzer ME. Osteochondral lesions of the talus: localization and morphologic data from 424 patients using a novel anatomical grid scheme. Foot Ankle Int. 2007;28(2):154-61.
7. Hepple S, Winson IG, Glew D. Osteochondral lesions of the talus: a revised classification. Foot Ankle Int. 1999;20(12):789-93.
8. Koo TK, Li MY. A Guideline of Selecting and Reporting Intraclass Correlation Coefficients for Reliability Research. J Chiropr Med. 2016;15(2):155-63.
9. Landis JR, Koch GG. The measurement of observer agreement for categorical data. Biometrics. 1977;33(1):159-74.
10. Martijn HA, Lambers KTA, Dahmen J, Stufkens SAS, Kerkhoffs GMMJ. High incidence of (osteo)chondral lesions in ankle fractures. Knee Surg Sports Traumatol Arthrosc. 2021;29(5):1523-1534.
11. Mann TS, Nery C. Osteochondral Lesion of the Talus: Quality of Life, Lesion Site, and Lesion Size. Foot Ankle Clin. 2024;29(2):213-224.
12. van Diepen PR, Dahmen J, Altink JN, Stufkens SAS, Kerkhoffs GMMJ. Location Distribution of 2,087 Osteochondral Lesions of the Talus. Cartilage. 2021 Dec;13(1_suppl):1344S-1353S.
13. van Dijk CN, Kennedy JG. Talar osteochondral defects: Diagnosis, planning, treatment, and rehabilitation. Talar Osteochondral Defects: Diagnosis, Planning, Treatment, and Rehabilitation. 2014 Jan 1;1–155.
14. Kessler JI, Weiss JM, Nikizad H, Gyurdzhyan S, Jacobs JC Jr, Bebchuk JD, et al. Osteochondritis dissecans of the ankle in children and adolescents: demographics and epidemiology. Am J Sports Med. 2014;42(9):2165-71.
15. Togher CJ, Sahli H, Butterfield J, Sebag J, Shane AM, Reeves CL. Incidence of Talar Osteochondral Lesions After Acute Ankle Fracture: A Retrospective Analysis. J Foot Ankle Surg. 2021;60(6):1184-1187.
16. Irwin RM, Shimozono Y, Yasui Y, Megill R, Deyer TW, Kennedy JG. Incidence of Coexisting Talar and Tibial Osteochondral Lesions Correlates With Patient Age and Lesion Location. Orthop J Sports Med. 2018;6(8):2325967118790965.
17. Chu IT, Kim YS, Yoo SH, Oh IS. The Incidences and Locations of Osteochondral Lesions of the Talus in Ankle Fracture. J Korean Orthop Assoc. 2004;39(5):494-497.

Abbreviations List

TOLs - Osteochondral lesions of the talusAA: aaaa
MRI - Magnetic resonance imaging
ROI - Region of interest
ICC - Intraclass correlation coefficient
PDw -Proton density-weighted
SPIR- Spectral presaturation inversion recovery sequences,
TSE- Turbo spin-echo sequences
PACS- Picture archiving and communication system

Ethics Approval and Consent to Participate

Antalya Training and Research Hospital institutional review board approved the study protocol (01/16, 06.01.2022).

Consent for Publication

Informed consent was obtained from the participants.

Availability of Data and Materials

Data sets generated during the current study are available from the corresponding author upon reasonable request.

Competing Interests

The authors declare that there are no financial or non-financial competing interests related to this study.

Funding

No funds have been received for this study.

Author Contributions

Idea/ Conception – F.D., M.Y.., Ö.K.; Design - F.D., M.Y.., Ö.K.;; Supervision - A.Y., F.D., M.Y.., Ö.K.;. ; Resources – A.Y..,M.B.E.,K.K.K., F.D.; Materials – M.Y., K.K.K.., M.B.E., F.D.; Data Collection and/or Processing - M.Y., K.K.K.., A.Y.., F.D.; Analysis and/or Interpretation – A.Y. Ö.K.; Literature Search - M.Y., K.K.K.., M.B.E., F.D., Ö.K.; Writing Manuscript – F.D., M.Y.., Ö.K.; Critical Review – A.Y., M.Y., K.K.K.., M.B.E., F.D., Ö.K.; Final approval of the version to be published- A.Y., M.Y., K.K.K.., M.B.E., F.D., Ö.K.

Acknowledgements

None.